Aerotecnica Missili & Spazio, *The Journal of Aerospace Science, Technology and Systems*

Performance Analysis and Gains Tuning Procedure for a Controlled Space Manipulator Used for Non-cooperative Target Capture Operations

A. Stolfi[a], P. Gasbarri[a], M. Sabatini[b]

[a] "Sapienza" - Università di Roma
Dipartimento di Ingegneria Meccanica e Aerospaziale

[b] "Sapienza" - Università di Roma
Dipartimento di Ingegneria Elettrica, Energetica e Astronautica

Abstract

In the near future robotic systems will be playing an increasingly important role in space applications such as repairing, refuelling, re-orbiting spacecraft and cleaning up the increasing amount of space debris. Space Manipulator Systems (SMSs) are robotic systems made of a bus (which has its own actuators such as thrusters and reaction wheels) equipped with one or more deployable arms. The present paper focuses on the issue of maintaining a stable first contact between the arms terminal parts (i.e. the end-effectors) and a non-cooperative target satellite, before the actual grasp is accomplished. The selected approach is a modified version of the Impedance Control algorithm, in which the end-effector is commanded in order to make it behave like a mass-spring-damper system regardless of the reaction motion of the base, so to absorb the impact energy. A very important aspect in the analysis of the control performance is the evaluation of the field of applicability of the controller itself. In the present work the influence of this issue on the effectiveness of the proposed control architecture will be analysed, together with the control gains tuning which allows for a robust achievement of the mission requirements. Several numerical results will be presented and discussed.

1. Introduction

The increasing number of launched satellites per year calls for solutions to keep free operational space for telecommunication systems in geo-synchronized orbit as well as to avoid the endangering of space systems in LEO (Low-Earth Orbit). One example for such dangerous stranded space systems is the uncontrolled and accidental de-orbiting of a huge satellite like ENVISAT. A feasible way to handle these problems might be to enforce the operational requirement to use some dedicated residual fuel for a controlled de-orbiting or, in case of GEO (Geostationary Orbit) satellites, to lift the latter at their end-of-life into a graveyard orbit. Despite these measures, malfunctions of solar panels, control systems or thrusters cannot be avoided. Therefore, on-orbit servicing will be a mandatory and challenging topic for space robotics in the near future. In this frame, researchers have suggested that robots will be crucial components of future orbital missions [1]. Although robotic systems have many limitations, they offer important advantages to augment, or in some cases replace, astronauts' capabilities in orbit. Robots have lower cost, require minimal support infrastructure and have an indefinite work life in orbit. In space missions such as the on-orbit servicing [2] or the active debris removal and the asteroid exploration, the control of contact forces between two bodies represents a big challenge for mission success, especially when autonomous robotic systems are employed. In fact the contact forces and, of course, the relative motion between two objects must be controlled carefully so as to avoid unexpected collision and/or damage on the robotic systems, i.e. the chaser satellite and the target satellite as well. Many researches have been studying the full control of contact phenomena, especially for an on-ground use [3-6]. Indeed, on-ground controls face the situation that both the environment/object and the base of a manipulator are constrained, which allows a long contact duration. However, on-orbit controls have to deal with contact between an unconstrained environment/object and a free-flying manipulator, which is a completely different context from that of on-ground operations. In fact, a Space Manipulator System (SMS) must be considered a floating system because its base is not fixed to the ground like the terrestrial ones. Therefore, the motion of the robotic arms affects the attitude and position of the base platform and vice versa. This is, of course,

particularly evident when both the base platform and the robotic arms have mass and inertia properties of the same order of magnitude. Such a "dynamic coupling" between the manipulator arms and the base platform makes the dynamics modelling and motion planning of a space robot much more complicated than those of fixed-base manipulators [7]. Recently the Authors of the present work investigated the application of the Impedance Control approach applied to a two-arm space manipulator to de-tumble and eventually capture a non-cooperative target [8]. Interest in this application is proved by other studies such as the one performed in [9] where a hybrid impedance/position control of a free-flying space robot for de-tumbling a non-cooperative satellite was proposed by using a single serial-link manipulator. The present paper focuses on the issue of maintaining a stable first contact between the arms terminal parts (i.e. the end-effectors) and a non-cooperative target satellite, before the actual grasp is performed, by using a modified version of the Impedance Control algorithm. Two arms, symmetrically mounted on a free-floating base platform, will be employed. It is worth to note that a very important aspect in the analysis of the control performance is the evaluation of the field of applicability of the controller itself. In the present work the influence of this issue on the effectiveness of the proposed control architecture will be analysed, together with the control gains tuning which allows for a robust achievement of the mission requirements. The control performance and the gains tuning procedure will be studied by means of a co-simulation involving the MSC Adams multibody code (for describing the dynamics of the space robot and target) together with Simulink (for the determination of the control actions). The paper is organized as follows: in Section 2 a brief overview of a multibody approach based on Kane's formulation is introduced to describe the dynamics of a two-arm space manipulator. In Section 3 the Impedance Control algorithm applied to a floating-base robotic system is described and the relevant mathematics is illustrated. In Section 4 several numerical results are presented whereas the final conclusions are reported in Section 5.

2. Multibody space robotic manipulator

In this section the multibody equations that describe the dynamics of the space manipulator will be briefly recalled. Indeed, the analytical details can be found in [8]. One of the possible approaches to derive the dynamic equations of a space manipulator, consisting of a base platform and one or more chains of links connected with each other through revolute joints, is by using a multibody formulation [10-12]. In this work the procedure to obtain the governing equations of the multibody space manipulator is based on Kane's formulation [13]. All the mathematics is derived in a 2D inertial reference frame, i.e. the motion of the space manipulator and the target is planar; in particular, the origin of this frame is located at the position of the SMS base centre of mass at $t = 0$ (see Figure 1). First, the Jacobian matrix $\mathbf{J}$ must be introduced. This matrix relates the time derivative of the Newtonian state vector with that of the minimum set of Lagrangian variables $\boldsymbol{Q}$. Here $\boldsymbol{Q}$ is the vector containing the base position and attitude variables, the arms joint angles and the distances of the centres of mass of the end-effectors contact plates from the end-point of the corresponding arm last link (see Figure 2). The governing equation of the space manipulator reads as follows [8]:

$$\mathbf{J}^{\mathrm{T}}\mathbf{M}\mathbf{J}\ddot{\boldsymbol{Q}} = \mathbf{J}^{\mathrm{T}}\boldsymbol{C} + \mathbf{J}^{\mathrm{T}}\boldsymbol{F} - \mathbf{J}^{\mathrm{T}}\mathbf{M}\dot{\mathbf{J}}\dot{\boldsymbol{Q}} \tag{1}$$

where $\mathbf{M}$ is the generalized mass matrix, $\boldsymbol{C}$ is the vector containing the non-linear velocity terms and $\boldsymbol{F}$ is the vector of external generalized forces, if any.

2.1. Two-arm manipulator and target satellite description

In Figure 2 the schematic of the two-arm space manipulator and the target satellite is reported. Speaking about the SMS, the first link of each robotic arm is connected to the base platform by means of a revolute joint and the links are connected with each other by revolute joints as well. The two end-effectors are formed by a spring-damper and a contact plate which is connected to the last link of the corresponding arm by means of a prismatic joint, i.e. it can only translate relatively to the last link (see Figure 3). Further details on the motivation for choosing this special configuration for the end-effector will be reported in the following. In Table 1 the geometrical and inertial properties of the links forming the two arms are indicated (the moment of inertia J_{J} is referred to the link left-end revolute joint). As far as the base platform is concerned, it has a cubic shape of length 1 m, its mass is $m_{\mathrm{b}} = 500\,\mathrm{kg}$ and its moment of inertia around the z axis of the centre of mass body-fixed reference frame is $J_{\mathrm{b}} = 83.33\,\mathrm{kgm}^2$. The contact plate reported in Figure 2 is 0.1 m high, with a mass of 0.35 kg and a moment

Table 1
Properties of the links of the space manipulator

Link	Mass (kg)	Length (m)	J_{J} (kgm^2)
1	20.00	1.10	6.93
2	20.00	1.10	6.93
3	19.27	1.05	6.56

of inertia of $2.95 \cdot 10^{-4}\,\mathrm{kgm}^2$. The end-effector spring length at rest is 0.2 m while the spring stiffness and damper damping coefficients are respectively equal to $3 \cdot 10^4\,\mathrm{N/m}$ and 200 Ns/m. The mass of the target satellite is 2721 kg and its moment of inertia around the z axis of the centre of mass body-fixed reference frame is $7895\,\mathrm{kgm}^2$.

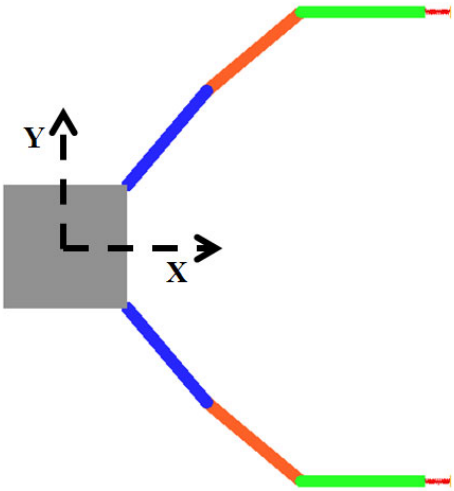

Figure 1. Schematic of the multibody space manipulator and the adopted inertial reference frame

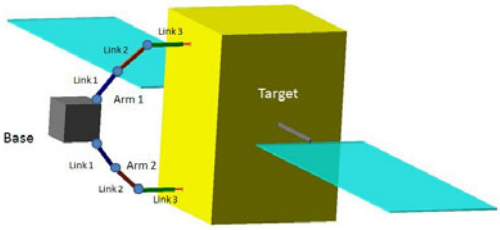

Figure 2. Schematic of the multibody space manipulator and the target satellite

3. Impedance Control algorithm for a space manipulator

Impedance Control provides compliant behaviour of a manipulator in dynamic interaction with its environment. Indeed, the impedance controller enforces a

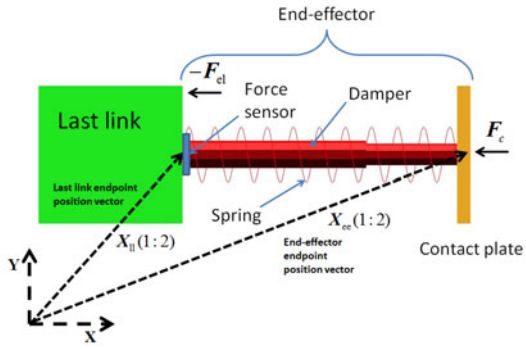

Figure 3. Schematic of the end-effector

relationship between the forces and moments acting on the manipulator end-effector and the acceleration, velocity and position errors of the end-effector itself (of course, with error the deviation from a desired value is intended). The impedance approach here used is based on an extended formulation of the original approach proposed by Yoshida et Al. in [14-15]. It considers a two-arm free-floating manipulator system with a particular emphasis to the impact and post-impact phases with an external target satellite. Furthermore, two-dimensional contact dynamics is taken into account as well. Again, the details of the mathematical formulation are not reported here for the sake of brevity and can be found in [8]. Suffices here to say that, before defining the Impedance Control algorithm, it is necessary to introduce the control actions into the dynamic governing equations, which must be written as:

$$\mathbf{J}^{\mathrm{T}}\mathbf{M}\mathbf{J}\ddot{\boldsymbol{Q}} = \mathbf{J}^{\mathrm{T}}\boldsymbol{C} + \mathbf{J}^{\mathrm{T}}\boldsymbol{F} - \mathbf{J}^{\mathrm{T}}\mathbf{M}\dot{\mathbf{J}}\dot{\boldsymbol{Q}} + \sum_{i=1}^{N_C}\mathbf{B}_i\boldsymbol{u}_i \quad (2)$$

where N_C is the number of control vectors, $\boldsymbol{u}_i$ is the i-th control vector and $\mathbf{B}_i$ is the matrix that maps the i-th control vector onto the dynamics equations. It has to be noticed that the vector $\mathbf{B}_i\boldsymbol{u}_i$ is not pre-multiplied by the transposed Jacobian matrix $\mathbf{J}^{\mathrm{T}}$ since the control actions are the ones referred to the minimal variables; if they had been referred to the Newtonian variables, they would have had to be pre-multiplied by $\mathbf{J}^{\mathrm{T}}$. The mission scenario is that of a target satellite approaching the manipulator system; the goal is to maintain a stable contact between the manipulator endpoints and the target satellite after the first contact has occurred. On account of this, the Impedance Control law is defined as:

$$\begin{aligned}&\mathbf{M}_{\mathrm{i}_k}\ddot{\boldsymbol{X}}_{\mathrm{ee}_k} + \mathbf{D}_{\mathrm{i}_k}\left(\dot{\boldsymbol{X}}_{\mathrm{ee}_k} - \dot{\boldsymbol{X}}_{\mathrm{ee}_{\mathrm{des}_k}}\right) + \\ &\mathbf{K}_{\mathrm{i}_k}\left(\boldsymbol{X}_{\mathrm{ee}_k} - \boldsymbol{X}_{\mathrm{ee}_{\mathrm{des}_k}}\right) = \boldsymbol{A}_{\mathrm{c}_k},\ \ k = 1,2\end{aligned} \quad (3)$$

where $\ddot{\boldsymbol{X}}_{\mathrm{ee}_k} \in \mathbb{R}^{3\times1}$, $\dot{\boldsymbol{X}}_{\mathrm{ee}_k} \in \mathbb{R}^{3\times1}$, $\boldsymbol{X}_{\mathrm{ee}_k} \in \mathbb{R}^{3\times1}$ are respectively the k-th end-effector endpoint acceleration, velocity and position (translational and angular ones (actually the angular ones are those of the end-effector itself)), $\dot{\boldsymbol{X}}_{\mathrm{ee}_{\mathrm{des}_k}} \in \mathbb{R}^{3\times1}$, $\boldsymbol{X}_{\mathrm{ee}_{\mathrm{des}_k}} \in \mathbb{R}^{3\times1}$ are their desired values, $\mathbf{M}_{\mathrm{i}_k} \in \mathbb{R}^{3\times3}$, $\mathbf{D}_{\mathrm{i}_k} \in \mathbb{R}^{3\times3}$, $\mathbf{K}_{\mathrm{i}_k} \in \mathbb{R}^{3\times3}$ are the Impedance Control matrices and $\boldsymbol{A}_{\mathrm{c}_k} \in \mathbb{R}^{3\times1}$ are the contact actions exerted on the k-th end-effector by the target satellite. More in detail, the Impedance Control matrices, differing from what has been done in [8], are chosen of the form:

$$\begin{aligned}
\mathbf{M}_{\mathrm{i}_k} &= \begin{pmatrix} m_{\mathrm{i}_{\mathrm{T}_k}} & 0 & 0 \\ 0 & m_{\mathrm{i}_{\mathrm{T}_k}} & 0 \\ 0 & 0 & m_{\mathrm{i}_{\mathrm{R}_k}} \end{pmatrix}, \\
\mathbf{D}_{\mathrm{i}_k} &= \begin{pmatrix} c_{\mathrm{i}_{\mathrm{T}_k}} & 0 & 0 \\ 0 & c_{\mathrm{i}_{\mathrm{T}_k}} & 0 \\ 0 & 0 & c_{\mathrm{i}_{\mathrm{R}_k}} \end{pmatrix}, \\
\mathbf{K}_{\mathrm{i}_k} &= \begin{pmatrix} k_{\mathrm{i}_{\mathrm{T}_k}} & 0 & 0 \\ 0 & k_{\mathrm{i}_{\mathrm{T}_k}} & 0 \\ 0 & 0 & k_{\mathrm{i}_{\mathrm{R}_k}} \end{pmatrix}
\end{aligned} \tag{4}$$

with different coefficients for the translational and rotational parts. This allows for a higher operational flexibility in dealing with the target satellite initial kinematic conditions. To better guarantee the control effectiveness and to increase the duration of contact between end-effector and target, it can be useful to place a spring-damper group between the arm last link and the end-effector contact plate as shown in Figure 3. On account of this choice, it is convenient to consider the last link endpoint rather than the end-effector endpoint as the controlled point so to avoid the presence of passive elements (represented by the spring-damper group) between the actuators and the controlled point. Considering this, Equation (3) is modified to become:

$$\begin{aligned}
&\mathbf{M}_{\mathrm{i}_k} \ddot{\boldsymbol{X}}_{\mathrm{ll}_k} + \mathbf{D}_{\mathrm{i}_k} \left(\dot{\boldsymbol{X}}_{\mathrm{ll}_k} - \dot{\boldsymbol{X}}_{\mathrm{ll}_{\mathrm{des}_k}} \right) + \\
&\mathbf{K}_{\mathrm{i}_k} \left(\boldsymbol{X}_{\mathrm{ll}_k} - \boldsymbol{X}_{\mathrm{ll}_{\mathrm{des}_k}} \right) = -\boldsymbol{A}_{\mathrm{el}_k},\ k = 1, 2
\end{aligned} \tag{5}$$

where $\ddot{\boldsymbol{X}}_{\mathrm{ll}_k} \in \mathbb{R}^{3\times1}$, $\dot{\boldsymbol{X}}_{\mathrm{ll}_k} \in \mathbb{R}^{3\times1}$, $\boldsymbol{X}_{\mathrm{ll}_k} \in \mathbb{R}^{3\times1}$ are respectively the k-th arm last link endpoint acceleration, velocity and position (translational and angular ones (the angular ones are those of the last link itself)) and $-\boldsymbol{A}_{\mathrm{el}_k} \in \mathbb{R}^{3\times1}$ are the spring-damper actions acting on the last link of the k-th arm. A further step consists in expressing the variables characterizing the last link endpoint position and orientation as a function of the set of Kane's variables. This is done by means of a Jacobian matrix $\mathbf{J}_{\mathrm{ll}_k} \in \mathbb{R}^{3\times\left(8+n_{\mathrm{l}_1}+n_{\mathrm{l}_2}\right)}$ (where n_{l_1} and n_{l_2} are the number of links forming the first and second arm respectively). Once again, the relevant algebra is not reported here for the sake of brevity. One finally gets:

$$\begin{aligned}
\ddot{\boldsymbol{Q}}_k = &-(\mathbf{M}_{\mathrm{i}_k}\mathbf{J}_{\mathrm{ll}_k})^{+} \left[\mathbf{M}_{\mathrm{i}_k}\dot{\mathbf{J}}_{\mathrm{ll}_k}\dot{\boldsymbol{Q}} + \mathbf{D}_{\mathrm{i}_k} \left(\mathbf{J}_{\mathrm{ll}_k}\dot{\boldsymbol{Q}} - \dot{\boldsymbol{X}}_{\mathrm{ll}_{\mathrm{des}_k}} \right) \right] \\
&-(\mathbf{M}_{\mathrm{i}_k}\mathbf{J}_{\mathrm{ll}_k})^{+} \left[\mathbf{K}_{\mathrm{i}_k} \left(\boldsymbol{X}_{\mathrm{ll}_k} - \boldsymbol{X}_{\mathrm{ll}_{\mathrm{des}_k}} \right) + \boldsymbol{A}_{\mathrm{el}_k} \right],\ k = 1, 2
\end{aligned} \tag{6}$$

where the + superscript indicates the pseudo-inversion operation. Equation (5) represents the synthetic control: it is the behaviour to be imposed on the last link endpoint variables to make it behave as if it was a mass-spring-damper system regardless of the reaction motion of the base. The concept of the Impedance Control approach is illustrated in Figure 4.

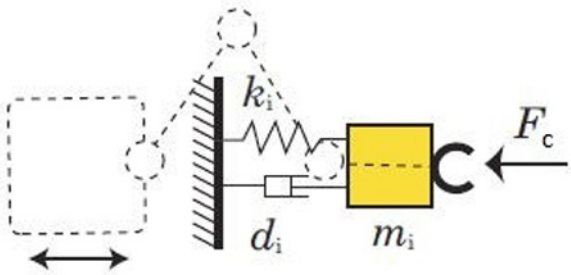

Figure 4. Impedance Control concept for a space manipulator [14]

Note that the end-effector spring-damper group represented in Figure 3 exists for real; it does not correspond to the imaginary spring and damper of the Impedance Control reported in Figure 4. It is worth underlining that Impedance Control does not impose any explicit requirements on the base platform behaviour. This could be not acceptable in the cases when translational and rotational constraints on the base motion need to be satisfied. To cope with this issue, a separate Proportional-Derivative (PD) Control strategy is applied to the SMS base. Defining

$$\boldsymbol{X}_{\mathrm{B}} = [x_{\mathrm{B}}, y_{\mathrm{B}}, \theta_{\mathrm{B}}]^{\mathrm{T}}$$

(i.e. the state vector of the base), the PD synthetic control law is given by

$$\ddot{\boldsymbol{X}}_{\mathrm{B}} = -\mathbf{K}_{\mathrm{p}} \left(\boldsymbol{X}_{\mathrm{B}} - \boldsymbol{X}_{\mathrm{B}_{\mathrm{des}}} \right) - \mathbf{K}_{\mathrm{d}} \left(\dot{\boldsymbol{X}}_{\mathrm{B}} - \dot{\boldsymbol{X}}_{\mathrm{B}_{\mathrm{des}}} \right) \tag{7}$$

where $\mathbf{K}_{\mathrm{p}} \in \mathbb{R}^{3\times3}$ and $\mathbf{K}_{\mathrm{d}} \in \mathbb{R}^{3\times3}$ are respectively the control proportional and derivative gain matrices chosen to be of the form:

$$\mathbf{K}_{\mathrm{p}} = \begin{pmatrix} K_{\mathrm{p_T}} & 0 & 0 \\ 0 & K_{\mathrm{p_T}} & 0 \\ 0 & 0 & K_{\mathrm{p_R}} \end{pmatrix}, \quad \mathbf{K}_{\mathrm{d}} = \begin{pmatrix} K_{\mathrm{d_T}} & 0 & 0 \\ 0 & K_{\mathrm{d_T}} & 0 \\ 0 & 0 & K_{\mathrm{d_R}} \end{pmatrix} \tag{8}$$

again with different coefficients for the translational and rotational controls. Of course, also in this case the vector $\dot{\boldsymbol{X}}_{\mathrm{B}}$ must be expressed in terms of the vector $\dot{\boldsymbol{Q}}$ by means of a Jacobian matrix $\mathbf{J}_{\mathrm{B}} \in \mathbb{R}^{3\times\left(8+n_{l_1}+n_{l_2}\right)}$. Equation (7) leads to:

$$\ddot{\boldsymbol{Q}} = -\mathbf{J}_{\mathrm{B}}^{+}\left[\mathbf{K}_{\mathrm{p}}\left(\boldsymbol{X}_{\mathrm{B}} - \boldsymbol{X}_{\mathrm{B_{des}}}\right) + \mathbf{K}_{\mathrm{d}}\left(\dot{\boldsymbol{X}}_{\mathrm{B}} - \dot{\boldsymbol{X}}_{\mathrm{B_{des}}}\right)\right] \tag{9}$$

In the following, the overall control strategy will be referred to as Impedance+PD Control.

3.1. Control actions

The control actions here considered are two forces acting on the base along the base x and y body axes (which are parallel to the base edges), a torque acting on the base around the base z body axis (which is parallel to the z inertial axis) and a number of torques equal to the number of joint motors whose axes are parallel to the z inertial axis. The base control actions will participate to the base PD Control while the joint torques of arm 1 and 2 will respectively contribute to the Impedance Control of the corresponding last link.

3.2. Governing equations of the Multibody Space Manipulator and target satellite

Kane's governing equations describing the controlled dynamics of the SMS and the target satellite (i.e. Equation (2) properly augmented to include the target dynamics as well) can be finally written in the following form:

$$\mathbf{J}^{\mathrm{T}}\mathbf{M}\mathbf{J}\ddot{\boldsymbol{Q}} = \mathbf{J}^{\mathrm{T}}\boldsymbol{C} + \mathbf{J}^{\mathrm{T}}\boldsymbol{F} - \mathbf{J}^{\mathrm{T}}\mathbf{M}\dot{\mathbf{J}}\dot{\boldsymbol{Q}} + \mathbf{B}_1\boldsymbol{u}_1 + \mathbf{B}_2\boldsymbol{u}_2 + \mathbf{B}_3\boldsymbol{u}_3 \tag{10}$$

The terms $\mathbf{B}_1 \in \mathbb{R}^{\left(8+n_{l_1}+n_{l_2}\right)\times n_{l_1}}$, $\mathbf{B}_2 \in \mathbb{R}^{\left(8+n_{l_1}+n_{l_2}\right)\times n_{l_2}}$, $\mathbf{B}_3 \in \mathbb{R}^{\left(8+n_{l_1}+n_{l_2}\right)\times 3}$ are the matrices that map the control actions vectors onto the dynamics equations. Separately substituting the desired accelerations appearing in Equations (6) and (9) into Equation (10), one obtains the vectors of generalized control forces [8]:

$$\begin{aligned} \boldsymbol{u}_1 &= \mathbf{B}_1^{+}\left\{\boldsymbol{\Gamma}_1\left[-\mathbf{M}_{\mathrm{i}_1}\dot{\mathbf{J}}_{\mathrm{ll}_1}\dot{\boldsymbol{Q}} - \mathbf{D}_{\mathrm{i}_1}(\dot{\boldsymbol{X}}_{\mathrm{ll}_1} - \dot{\boldsymbol{X}}_{\mathrm{ll}_{\mathrm{des}_1}})\right]\right\} + \\ &+ \mathbf{B}_1^{+}\left\{\boldsymbol{\Gamma}_1\left[-\mathbf{K}_{\mathrm{i}1}(\boldsymbol{X}_{\mathrm{ll}_1} - \boldsymbol{X}_{\mathrm{ll}_{\mathrm{des}_1}}) - \boldsymbol{A}_{\mathrm{el}_1}\right]\right\} + \\ &+ \mathbf{B}_1^{+}\left\{\mathbf{J}^{\mathrm{T}}\mathbf{M}\dot{\mathbf{J}}\dot{\boldsymbol{Q}} - \mathbf{J}^{\mathrm{T}}\boldsymbol{C} - \mathbf{J}^{\mathrm{T}}\boldsymbol{F}'\right\} \end{aligned} \tag{11}$$

$$\begin{aligned} \boldsymbol{u}_2 &= \mathbf{B}_2^{+}\left\{\boldsymbol{\Gamma}_2\left[-\mathbf{M}_{\mathrm{i}_2}\dot{\mathbf{J}}_{\mathrm{ll}_2}\dot{\boldsymbol{Q}} - \mathbf{D}_{\mathrm{i}_2}(\dot{\boldsymbol{X}}_{\mathrm{ll}_2} - \dot{\boldsymbol{X}}_{\mathrm{ll}_{\mathrm{des}_2}})\right]\right\} + \\ &+ \mathbf{B}_2^{+}\left\{\boldsymbol{\Gamma}_2\left[-\mathbf{K}_{\mathrm{i}_2}(\boldsymbol{X}_{\mathrm{ll}_2} - \boldsymbol{X}_{\mathrm{ll}_{\mathrm{des}_2}}) - \boldsymbol{A}_{\mathrm{el}_2}\right]\right\} + \\ &+ \mathbf{B}_2^{+}\left\{\mathbf{J}^{\mathrm{T}}\mathbf{M}\dot{\mathbf{J}}\dot{\boldsymbol{Q}} - \mathbf{J}^{\mathrm{T}}\boldsymbol{C} - \mathbf{J}^{\mathrm{T}}\boldsymbol{F}'\right\} \end{aligned} \tag{12}$$

$$\begin{aligned} \boldsymbol{u}_3 &= \mathbf{B}_3^{+}\left\{\boldsymbol{\Gamma}_3\left[-\mathbf{K}_{\mathrm{p}}(\boldsymbol{X}_{\mathrm{B}} - \boldsymbol{X}_{\mathrm{B_{des}}}) - \mathbf{K}_{\mathrm{d}}(\dot{\boldsymbol{X}}_{\mathrm{B}} - \dot{\boldsymbol{X}}_{\mathrm{B_{des}}})\right]\right\} + \\ &+ \mathbf{B}_3^{+}\left\{\mathbf{J}^{\mathrm{T}}\mathbf{M}\dot{\mathbf{J}}\dot{\boldsymbol{Q}} - \mathbf{J}^{\mathrm{T}}\boldsymbol{C} - \mathbf{J}^{\mathrm{T}}\boldsymbol{F}'\right\} \end{aligned} \tag{13}$$

where

$$\begin{aligned} \boldsymbol{\Gamma}_1 &= \mathbf{J}^{\mathrm{T}}\mathbf{M}\mathbf{J}(\mathbf{M}_{\mathrm{i}_1}\mathbf{J}_{\mathrm{ll}_1})^{+} \\ \boldsymbol{\Gamma}_2 &= \mathbf{J}^{\mathrm{T}}\mathbf{M}\mathbf{J}(\mathbf{M}_{\mathrm{i}_2}\mathbf{J}_{\mathrm{ll}_2})^{+} \\ \boldsymbol{\Gamma}_3 &= \mathbf{J}^{\mathrm{T}}\mathbf{M}\mathbf{J}\mathbf{J}_{\mathrm{B}}^{+} \end{aligned} \tag{14}$$

4. Numerical results

As mentioned in Section 1, we want to study the dynamic interaction of a space manipulator and a non-cooperative target orbiting nearby. In particular, we are interested in the contact and post-contact (pre-grasping) phases. As initial conditions, the arms of the SMS are already deployed and the end-effectors are very close to the target satellite. The SMS is at rest, with its centre of mass aligned along the x inertial axis with the target centre of mass. For what concerns the target, in the nominal case considered in the following, the translational velocity components with respect to the inertial reference frame are assumed as $V_{x_0} = -5\,\mathrm{cm/s}$ and $V_{y_0} = 0$ (the positive directions of the inertial axes are shown in Figure 1); it also has an angular velocity around its center of mass of $\omega_{z_0} = 1\,\mathrm{deg/s}$. As far as the desired values of the state variables appearing in the control vectors expressions are concerned, they are assumed to be equal to those of the initial conditions. In all the following simulations we have considered a duration time of the manoeuvre equal to 60 s. After this time interval, a new phase of the mission is supposed to take place where the grasping of the target with the use of mechanical grippers or robotic hands is involved (but this part is not analysed in the present work).

4.1. Control strategies effectiveness evaluation

The effectiveness of a control strategy in a pre-grasping operation can be positively evaluated when some requirements on the kinematic and dynamic state of the SMS and the target are satisfied (the adopted thresholds are reported within parentheses and are reasonable example values for this type of mission):

- The magnitude of the contact forces is sufficiently small ($\leq 1\,\mathrm{N}$);
- During the manoeuvre the distances between the end-effectors and the target are null or within a prescribed tolerance (of the order of centimetres);
- During the manoeuvre the SMS base shows relatively small translational displacement magnitude and angular displacements (respectively $\leq 5\,\mathrm{cm}$ and $\leq 2\,\mathrm{deg}$);
- The target translational velocity magnitude and angular velocity are smaller than prescribed design ones (respectively $\leq 0.5\,\mathrm{cm/s}$ and $\leq 0.05\,\mathrm{deg/s}$);
- Conditions 1 and 4 are maintained for a prescribed time interval (of the order of 10 s).

4.2. Control gains selection procedure

In all the following simulations the values of the SMS base PD Control are the ones obtained by the Authors in [8] by means of a parametric study there detailed.

4.2.1. Impedance Control gains parametric analysis

Contrary to [8], in the present work non-zero values for the Impedance Control virtual stiffness coefficients are considered. This, although on one hand can lead to better performances of the control strategy, on the other poses the issue of carefully choosing adequate combinations of the mass, damping and stiffness parameters in order to avoid a "spring-effect" behaviour on both the end-effectors that can potentially produce an unwanted early detachment of the target. All the tested gains combinations are reported in Table 2, where the check and cross symbols in the last column respectively indicate whether the mission requirements stated in Section 4.1 are satisfied or not. As it can be seen from Table 2, there are many gains sets which satisfy the mission requirements. In order to take into account the different variables of interest in the evaluation of the "best" control gains set, it is convenient to introduce a Cost Function J able to represent different aspects of the mission in terms of power consumption of the actuators, deviation from the required position of the base platform centre of mass and its attitude and the translational and angular velocities of the target. Since the above quantities are not homogenous, it is preferable to introduce weighting coefficients so that the Cost Function J is defined as follows:

$$J = P_1 e_{\mathrm{T}} + P_2 e_{\mathrm{R}} + P_3 u_{\mathrm{T}} + P_4 u_{\mathrm{R}} + P_5 u_{\mathrm{J}} + P_6 e_{\mathrm{T_t}} + P_7 e_{\mathrm{R_t}} \tag{15}$$

where P_i, $i = 1, ..., 7$ are properly chosen weighting parameters such that $P_i = P_{i_1} P_{i_2}$ where P_{i_1} are non-dimensionalization coefficients and P_{i_2} are the effective weights which are used to establish the relevance that wants to be assigned to the term they multiply. Namely, the latter are assumed as $P_{1_2} = P_{3_2} = P_{4_2} = P_{6_2} = P_{7_2} = 1$, $P_{2_2} = P_{5_2} = 10$ (this choice was made in order for the different terms appearing on the right-hand side of Equation (15) to be of the same order of magnitude). The other quantities appearing in the above relation are given by:

$$\begin{aligned}
e_{\mathrm{T}} &= \max \sqrt{e_{\mathrm{T}_x}^2 + e_{\mathrm{T}_y}^2} \\
e_{\mathrm{R}} &= \max \left| e_{\mathrm{R}_z} \right| \\
u_{\mathrm{T}} &= \mathrm{mean} \left| u_{\mathrm{T}_x} \right| + \mathrm{mean} \left| u_{\mathrm{T}_y} \right| \\
u_{\mathrm{R}} &= \mathrm{mean} \left| u_{\mathrm{R}_z} \right| \\
u_{\mathrm{J}} &= \sum_{k=1}^{n_{l_1}+n_{l_2}} \mathrm{mean} \left| u_{\mathrm{J}_{z_k}} \right| \\
e_{\mathrm{T_t}} &= \mathrm{mean} \sqrt{v_{\mathrm{t}_x}^2 + v_{\mathrm{t}_y}^2} \\
e_{\mathrm{R_t}} &= \mathrm{mean} \left| \omega_{\mathrm{t}_z} \right|
\end{aligned} \tag{16}$$

where e_{T_x} is the x inertial component of the SMS base centre of mass position deviation from the desired one, e_{T_y} is the y inertial component of the same entity, e_{R_z} is the deviation of the SMS base attitude angle with respect to the x inertial axis from the desired one, u_{T_x} is the control force component along the SMS base x body axis acting on the base, u_{T_y} is the y body component of the same quantity, u_{R_z} is the control torque (about the base z body axis) acting on the SMS base, $u_{\mathrm{J}_{z_k}}$ is the control torque (about the joint z axis) acting at the k-th joint, v_{t_x} and v_{t_y} are respectively the x and y inertial components of the target centre of mass velocity and ω_{t_z} is the target angular velocity (around the z inertial axis). The "best" set of gains is chosen as the one that minimizes the above defined cost function; in particular, the minimum is found for the gains set highlighted in red in Table 2. In the following simulations the latter is used for the Impedance Control of both the last links.

4.3. Analysis of the Impedance+PD Control performance and applicability range evaluation

4.3.1. Impedance+PD Control performance analysis

Taking into consideration the Impedance Control gains evaluated in Section 4.2, we are going to analyse the performance of the proposed control architecture in the nominal scenario. In Figure 5 a sketch of the evolution of the system is reported. It is possible to observe how the developed strategy makes the chaser able to absorb the impact and that at the end of the

Table 2
Analysed control gain parameters

m_{i_T}	c_{i_T}	k_{i_T}	m_{i_R}	c_{i_R}	k_{i_R}	$m_i : c_i : k_i$	Result
2.5	125	0.125	25	1250	1.25	1:50:0.05	√
2.5	125	0.625	25	1250	6.25	1:50:0.25	√
2.5	125	1.25	25	1250	12.5	1:50:0.5	√
2.5	125	1.875	25	1250	18.75	1:50:0.75	√
2.5	125	2.5	25	1250	25	1:50:1	×
2.5	125	3.125	25	1250	31.25	1:50:1.25	×
2.5	125	3.75	25	1250	37.5	1:50:1.5	×
10	**500**	**0.5**	**100**	**5000**	**5**	**1:50:0.05**	√
10	500	2.5	100	5000	25	1:50:0.25	√
10	500	5	100	5000	50	1:50:0.5	√
10	500	7.5	100	5000	75	1:50:0.75	√
10	500	10	100	5000	100	1:50:1	√
10	500	12.5	100	5000	125	1:50:1.25	√
10	500	15	100	5000	150	1:50:1.5	√
100	5000	5	1000	50000	50	1:50:0.05	√
100	5000	25	1000	50000	250	1:50:0.25	√
100	5000	50	1000	50000	500	1:50:0.5	√
100	5000	75	1000	50000	750	1:50:0.75	√
100	5000	100	1000	50000	1000	1:50:1	√
100	5000	125	1000	50000	1250	1:50:1.25	×
100	5000	150	1000	50000	1500	1:50:1.5	×
100	10000	5	1000	100000	50	1:100:0.05	×
100	10000	25	1000	100000	250	1:100:0.25	×
100	10000	50	1000	100000	500	1:100:0.5	×
100	10000	75	1000	100000	750	1:100:0.75	×
100	10000	100	1000	100000	1000	1:100:1	×
100	10000	125	1000	100000	1250	1:100:1.25	×
100	10000	150	1000	100000	1500	1:100:1.5	×
200	10000	10	2000	100000	100	1:50:0.05	×
200	10000	50	2000	100000	500	1:50:0.25	×
200	10000	100	2000	100000	1000	1:50:0.5	×
200	10000	150	2000	100000	1500	1:50:0.75	×
200	10000	200	2000	100000	2000	1:50:1	×
200	10000	250	2000	100000	2500	1:50:1.25	×
200	10000	300	2000	100000	3000	1:50:1.5	×

manoeuvre both the end-effectors of the SMS remain very close to the target satellite.

In Figure 6 the time history of the contact forces acting on the contact plates of the two end-effectors is also reported. The sharp variations in the two curves are indicative of the beginning of the contact phase between the bodies. It can be seen that for arm 1 the magnitude reaches a constant zero value from $t = 29.7\,\mathrm{s}$ on; an analogous thing happens for arm 2 starting from $t = 19.2\,\mathrm{s}$ on. This means that both the end-effectors have actually lost contact with the target. Nevertheless, it has been verified that the distances dividing the contact plates from the target bus display values which are below the threshold given for requirement ♯2 in Subsection 4.1. These considerations allow to say that the first two requirements are satisfied.

In Figures 7 and 8 the magnitude of the SMS base centre of mass displacement and the base attitude angle with respect to the x inertial axis are respectively reported. It can be noticed that these two variables are well below the maximum allowed ones which implies that the third requirement is satisfied as well. It is interesting to observe that both the curves show a periodic-like behaviour.

The kinematic behaviour of the target is shown in Figures 9 and 10. The target centre of mass velocity magnitude is reduced to much less than a tenth of its initial value and the target angular velocity practically to zero. So requirement ♯4 is verified.

As far as the fifth requirement is concerned, it can be said that it is functional to the successive grasping phase in the sense that the time interval could

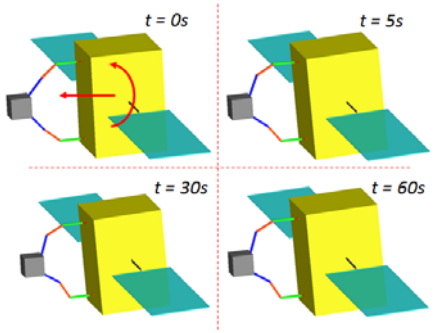

Figure 5. Sketch of the system dynamic evolution when Impedance+PD Control is applied (nominal case)

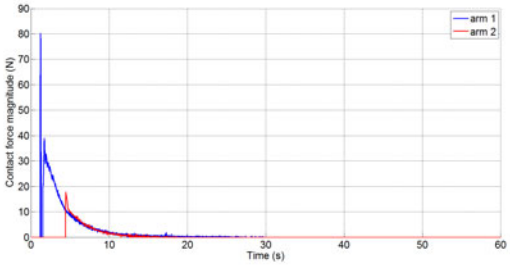

Figure 6. Magnitude of the contact forces acting between the SMS contact plates and the target (nominal case)

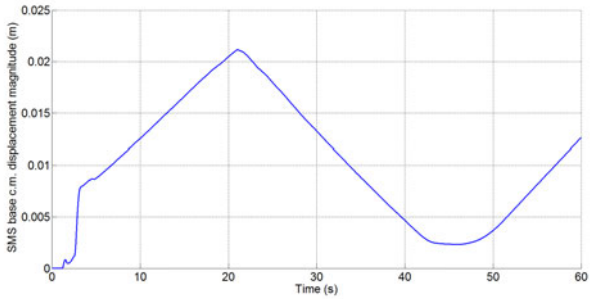

Figure 7. SMS base centre of mass displacement magnitude (nominal case)

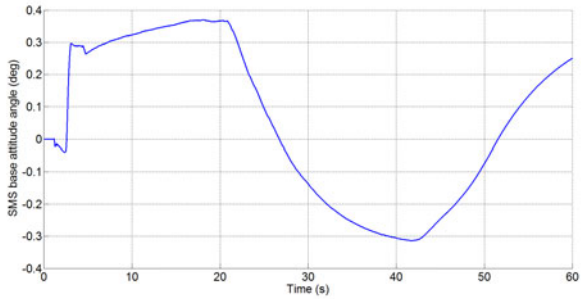

Figure 8. SMS base attitude angle with respect to the x inertial axis (nominal case)

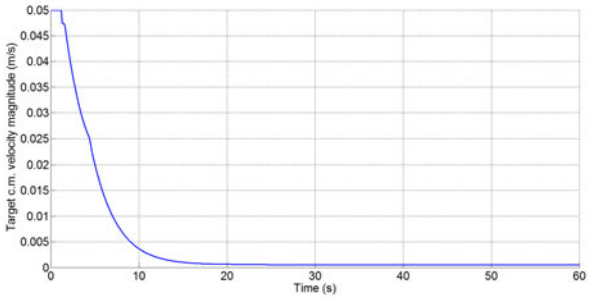

Figure 9. Target centre of mass velocity magnitude (nominal case)

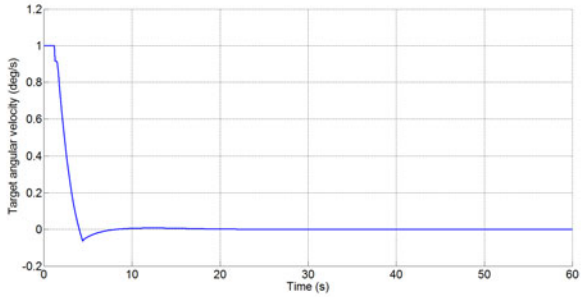

Figure 10. Target angular velocity (nominal case)

be, for example, the time necessary to the grippers to perform the grasping manoeuvre. From Figures 6, 9 and 10 it can be seen that requirements 1 and 4 are verified starting from $t = 20\,\mathrm{s}$ going on. Consequently, the grasping operation could begin at any time instant following $t = 20\,\mathrm{s}$.

4.3.2. Impedance+PD Control applicability range evaluation

It could well happen in actual on-orbit missions that the initial kinematic conditions of the target satellite

do not coincide with those considered in the nominal design. On account of this, it is interesting to evaluate the applicability range of the proposed Impedance+PD Control strategy given the optimal set of gains determined in the nominal conditions and varying the target satellite initial kinematic state. Table 3 shows the results of this analysis where in the first column and the first row the magnitude of the target centre of mass initial velocity and the target initial angular velocity are respectively reported. The check and cross symbols respectively indicate that the mission is either accomplished or not. Looking at the table it is possible to notice how the selected gains set is actually able to face a good number of out-of-design conditions, ranging from to 2.5 to 10 cm/s and from 0.5 to 2.5 deg/s. A relevant aspect that has been detected in this analysis - besides the values of the two variables taken separately - is their combination. In fact, it can be seen that high or low values for the target initial conditions could be sustainable or not according to the way they are reciprocally coupled.

Table 3
Impedance+PD Control applicability range evaluation

	0.5	1	1.5	2	2.5	3
2.5	√	√	×	×	×	×
5	√	√	√	√	×	×
7.5	√	√	√	√	√	×
10	×	√	√	×	×	×
12.5	×	×	×	×	×	×

In order to have a more quantitative idea of how the controller behaves in out-of-design conditions, in the following the results relative to the worst analysed case (i.e. 12.5 cm/s − 3 deg/s) are shown.

Figures from 11 to 16 show that requirement ♯1 is satisfied, but, on the other hand, requirements ♯2, 3, 4 and 5 are not. Nevertheless, the reported values of the SMS base attitude angle and the target angular velocity violate just slightly the imposed constraints and those of the SMS base centre of mass displacement magnitude and the target centre of mass velocity magnitude remain of the same order of magnitude of the maximum allowed ones.

5. Conclusions

In this work the scenario of a two-arm Space Manipulator System and a target satellite coming in contact has been presented. An Impedance+PD Control algorithm has been developed to allow contact keeping between the manipulator end-effectors and the target without performing a real grasp. We evaluated the effectiveness of the proposed control architecture

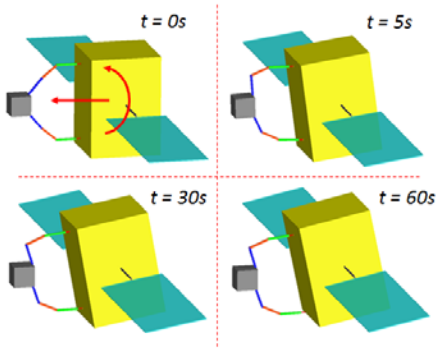

Figure 11. Sketch of the system dynamic evolution when Impedance+PD Control is applied (worst case)

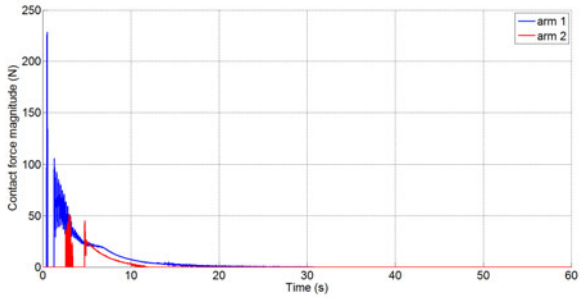

Figure 12. Magnitude of the contact forces acting between the SMS contact plates and the target (worst case)

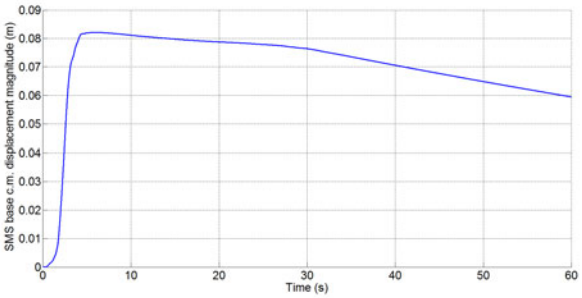

Figure 13. SMS base centre of mass displacement magnitude (worst case)

by means of a co-simulation involving the commercial multibody code MSC Adams and Simulink. Furthermore, an applicability range evaluation analysis

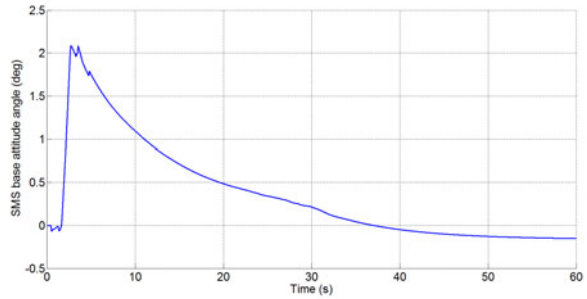

Figure 14. SMS base attitude angle with respect to the x inertial axis (worst case)

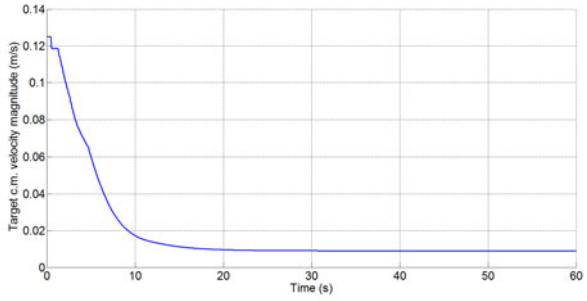

Figure 15. Target centre of mass velocity magnitude (worst case)

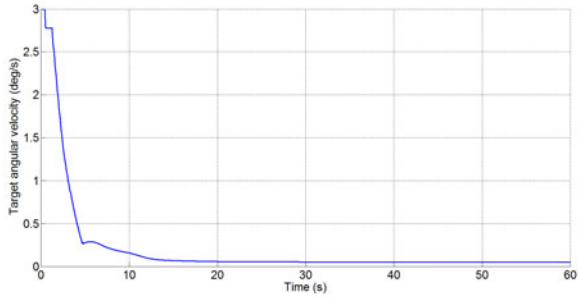

Figure 16. Target angular velocity (worst case)

has been conducted considering out-of-design values for the target initial kinematic conditions. As far as the choice of the gains for the Impedance Control of the arms last links is concerned, a parametric analysis has been performed introducing an opportunely defined cost function to be minimized. The obtained results allow to say that the developed control strategy is suitable for application in a pre-grasping manoeuvre satisfying the user-defined requirements and also showing a good applicability range.

REFERENCES

1. D. King, Space Servicing: Past, Present and Future, Proceedings of the 6th International Symposium on Artificial Intelligence and Robotics & Automation in Space, Montreal, Canada. 2001.
2. A. Flores-Abad, O. Ma, K. Pham, S. Ulrich, A review of space robotics technologies for on-orbit servicing, Progress Aerosp. Sci. 68 (2014), pp. 1-26.
3. N. Hogan, Impedance Control: An Approach to Manipulation: Part III - Applications, Journal of Dynamic Systems, Measurement and Control, Vol. 107, Issue 1 (1985).
4. M. Raibert, J. Craig, Hybrid Position/Force Control of Manipulators, ASME Journal of Dynamic Systems, Measurement and Control, Vol. 102, No. 2, 1981, pp. 126-133.
5. K. Kosuge, H. Yoshida, T. Fukuda, M. Sakai, K. Kanitani, K. Hariki, Unified control for dynamic cooperative manipulation, Intelligent Robots and Systems '94. Proceedings of the IEEE/RSJ/GI International Conference on, Vol. 2, 1994, pp. 1042-1047.
6. H. Sadeghian, F. Ficuciello, L. Villani, M. Keshmiri, Global Impedance Control of Dual-Arm Manipulation for Safe Interaction, IFAC Proceedings Volumes, Vol. 45, Issue 22, 2012, pp. 767-772.
7. P. Gasbarri, A. Pisculli, Dynamic/control interactions between flexible orbiting space-robot during grasping, docking and post-docking maneuvers, Acta Astronautica, Vol. 110, May-June 2015, pp. 225-238.
8. A. Stolfi, P. Gasbarri, M. Sabatini, A Combined Impedance-PD Approach for Controlling a Dual-Arm Space Manipulator in the Capture of a Non-Cooperative Target, Acta Astronautica, Vol. 139, October 2017, pp. 243-253.
9. N. Uyama, T. Narumi, Hybrid Impedance/Position Control of a Free-Flying Space Robot for Detumbling a Noncooperative Satellite, IFAC-Papers On Line, Vol. 49, Issue 17, 2016, pp. 230-235.
10. P. Santini, P. Gasbarri, Dynamics of Multibody Systems in Space Environment; Lagrangian vs. Eulerian Approach, Acta Astronautica, Vol. 54, Issue 1, Jan. 2004, pp. 1-24.
11. A.Pisculli, P. Gasbarri, A Minimum State Multibody/FEM Approach for Modeling Flexible Orbiting Space Systems, Acta Astronautica, Vol. 110, MayJune 2015, pp. 324-340.
12. A. Pisculli, L. Felicetti, P Gasbarri, G.B. Palmerini, M. Sabatini, A reaction-null/Jacobian transpose control strategy with gravity gradient compensation for on-orbit space manipulators, Aerospace Science and Technology, Vol. 38, October 2014, pp. 30-40.
13. T. Kane, D. Levinson, The use of Kane's dynamical equations in robotics, International Journal of Robotics Research, Vol. 2, No. 3, 1983, pp. 3-21.
14. H. Nakanishi, K. Yoshida, Impedance control for free-flying space robots - basic equations and applications, IEEE/RSJ international conference on intelligent robots and systems, Beijing, China, 2006, pp. 3137-42.
15. N. Uyama, H. Nakanishi, K. Nagaoka, K. Yoshida, Impedance-Based Contact Control of a Free-Flying Space Robot with a Compliant Wrist for Non-Cooperative Satellite Capture, 2012 IEEE/RSJ International Conference on Intelligent Robots and Systems, October 7-12, 2012, Vilamoura, Algarve, Portugal.